

# Deterministic and probabilistic analysis of tunnel face stability using support vector machine

Bin Li<sup>1</sup>, Yong Fu<sup>2</sup>, Yi Hong<sup>3</sup> and Zijun Cao<sup>\*4</sup>

<sup>1</sup>School of Transportation, Wuhan University of Technology, Hubei Highway Engineering Research Center, 1178 Heping Avenue, Wuhan, Hubei Province 430063, China

<sup>2</sup>Department of Ocean Science and Engineering, Southern University of Science and Technology, Shenzhen 518055, China

<sup>3</sup>College of Civil Engineering and Architecture, Zhejiang University, Hang Zhou, China

<sup>4</sup>State Key Laboratory of Water Resources and Hydropower Engineering Science, Key Laboratory of Rock Mechanics in Hydraulic Structural Engineering, Ministry of Education, Wuhan University, 8 Donghu South Road, Wuhan, China

(Received October 14, 2020, Revised February 6, 2021, Accepted February 18, 2021)

**Abstract.** This paper develops a convenient approach for deterministic and probabilistic evaluations of tunnel face stability using support vector machine classifiers. The proposed method is comprised of two major steps, i.e., construction of the training dataset and determination of instance-based classifiers. In step one, the orthogonal design is utilized to produce representative samples after the ranges and levels of the factors that influence tunnel face stability are specified. The training dataset is then labeled by two-dimensional strength reduction analyses embedded within OptumG2. For any unknown instance, the second step applies the training dataset for classification, which is achieved by an ad hoc Python program. The classification of unknown samples starts with selection of instance-based training samples using the k-nearest neighbors algorithm, followed by the construction of an instance-based SVM-KNN classifier. It eventually provides labels of the unknown instances, avoiding calculate its corresponding performance function. Probabilistic evaluations are performed by Monte Carlo simulation based on the SVM-KNN classifier. The ratio of the number of unstable samples to the total number of simulated samples is computed and is taken as the failure probability, which is validated and compared with the response surface method.

**Keywords:** tunnel face stability; support vector machine; the k-nearest neighbors; strength reduction analysis; Monte Carlo simulation

## 1. Introduction

Tunnel face stability is a major concern in tunnelling engineering because the instability of a tunnel face may severely threaten the safety of workers, equipment and existing nearby structures and utilities. Face collapse is very likely to happen at the construction stage for tunnels driven in soils. In these cases, stabilization measures are usually required for the purpose of prevention and control of active failure in front of the tunnel face. However, the application of such measures is often costly, time-consuming, and labor-intensive. Therefore, it is essential to predict where the face collapse may occur during the tunnel construction.

There are various analytical, experimental, and numerical methods for evaluations of tunnel face stability in the literature (Lee 2016, Khezri *et al.* 2016, Zhang *et al.* 2017, Li and Yang 2019a, b). Leca and Dormieux (1990) proposed a collapse mechanism composed of two truncated conical blocks to determine retaining pressures against face collapse and blow-out failure. The two-block failure mechanism was then improved to a multiblock collapse mechanism (Mollon *et al.* 2009a, Mollon *et al.* 2010), and then to a rotational failure mechanism (Mollon *et al.* 2011).

These methods need to prescribe a failure surface, and then establish and solve the governing equations with respect to tunnel face stability through the limit analysis method. In addition, centrifuge model tests have been used to study the face stability of tunnels, with the purpose of observing failure patterns and determining limit support pressures (Chambon and Corte 1994), validating the proposed analytical methods (Leca and Dormieux 1990), investigating failure mechanism (Wong *et al.* 2012), and checking the effects of auxiliary measures (Kamata and Mashimo 2003, Juneja *et al.* 2010). Recently, numerical methods have become popular in tunnel face stability analysis as it does not need to prescribe the failure surface prior to the analysis compared with the analytical methods, and has been shown to be a cost-effective tool for investigating the tunnel face stability. Simulations have been performed to evaluate the effects of reinforcements on preventing face collapse (Paternesi *et al.* 2017), or to design reinforcement parameters (Ng and Lee 2002, Dias 2011, Li *et al.* 2015).

Existing studies showed that tunnel face stability is mainly influenced by various factors, including, but not limited to, the material parameters of surrounding soils, the surcharge loading located on the ground surface, the cover depth, and the diameter of the tunnel (Leca and Dormieux 1990, Chambon and Corte 1994, Yamamoto *et al.* 2011, Anagnostou and Perazzelli 2013, Paternesi *et al.* 2017). In

\*Corresponding author, Professor, Ph.D.  
E-mail: [zijuncao@whu.edu.cn](mailto:zijuncao@whu.edu.cn)

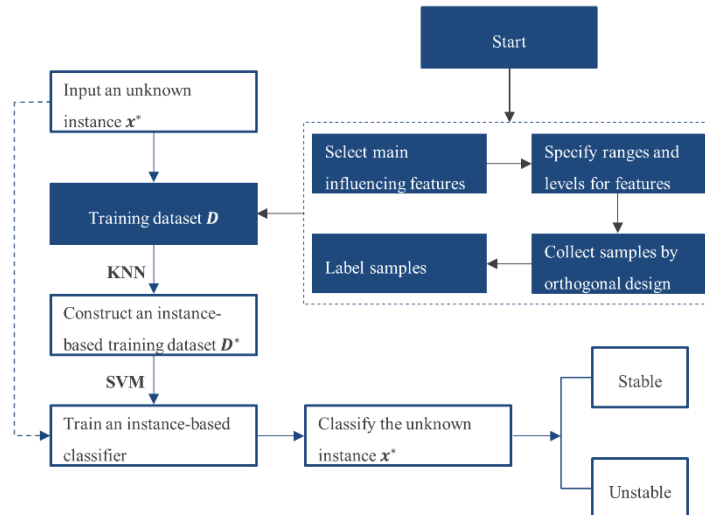


Fig. 1 Framework of the proposed SVM-KNN method for tunnel face stability analysis

practice, these factors usually vary from location to location, indicating that the states of tunnel face may change frequently along the axis of the tunnel. This means that one tunnel requires a number of evaluations of tunnel face stability for different cross sections, which is time-consuming for conventional methods. A load factor, called stable ratio or stability number (Klar *et al.* 2007, ITA/AITES 2007), is capable of estimating whether or not a tunnel face is stable with a great efficiency. However, this method is only limited to tunnels driven in purely cohesive soils. A more widely applicable approach that has comparable efficiency is still expected. Essentially, if the main purpose is to determine whether or not a tunnel face is stable, the deterministic evaluation task can be reformulated as a binary classification problem. In a similar spirit, a probabilistic evaluation can be converted to a certain number of binary classifications (Pan and Dias 2017). Various machine learning algorithms (Zhang and Goh 2014, 2016, Xiang *et al.* 2018, Zhang *et al.* 2018) like support vector machine (SVM) have been proven to be efficient in solving such types of problems (Pal 2006, Goh and Goh 2007, Bourinet *et al.* 2011, Samui and Karthikeyan 2013, Tinoco *et al.* 2014, Pham *et al.* 2016).

Given a training dataset, a machine learning model can be trained to classify unknown samples. The performance of the model relies on the quantity and quality of training data (or samples) (Chan *et al.* 2004). The training samples can be either derived from monitoring data of real-life projects or produced according to sampling design methods, such as uniform design (Li *et al.* 2016, Li and Yang 2019) and orthogonal design (Qiu *et al.* 2016, Xu *et al.* 2017). Generally, geometry parameters (e.g., the diameter of a tunnel) is usually not taken into account when choosing variables (Mahdevari *et al.* 2012, Shi *et al.* 2019, Zhang *et al.* 2019). The trained model is, therefore, not feasible to be used for cases with different geometry parameters.

To overcome the above limitation, this paper constructs a training dataset that includes sufficient labeled samples at the beginning and then selects suitable training samples from this dataset for the classification. The main factors that

influence tunnel face stability are taken into consideration when determining training samples, and the experimental domain to be defined wide enough to cover routine cases occurring in design practice. Beyond that, the technique of selection of suitable training samples is also very important. For a new data point, the k-nearest neighbors (KNN) algorithm is capable of searching the k-nearest data points, which has the shortest distances from the data point concerned. KNN was combined with SVM to develop a SVM-KNN method (Zhang *et al.* 2006), which has been proven to outperform the original SVM (Zhang *et al.* 2006, Li *et al.* 2008). This proposed SVM-KNN method is applicable to both deterministic and probabilistic evaluations of tunnel face stability, and it is comprised of two major steps: construction of the training dataset and determination of instance-based classifiers using SVM-KNN, which are described in detail as below.

## 2. Description of the method

### 2.1 General framework

Fig. 1 shows the proposed framework comprised of two major steps. The step one (represented by solid rectangles) constructs a training dataset (denoted by  $D$ ). The second step (represented by blank rectangles) applies the training dataset to perform classifications of tunnel face stability.

For an unknown instance (denoted by  $x^*$ ), KNN is employed to search the k nearest data points from the training dataset  $D$  to construct an instance-based training dataset  $D^*$ , which is then used to fit an instance-based model to classify the unknown instance  $x^*$ . Note that once the step one is completed, the next step can be readily repeated for different unknown instances. This enables one to perform a large number of predictions in a cost-effective manner. More importantly, with the trained model, probabilistic analysis of tunnel face stability becomes trivial by performing classifications for a set of instances (or

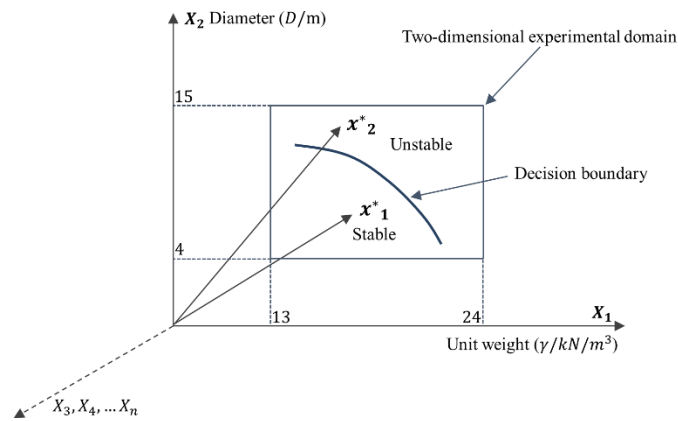


Fig. 2 Schematic diagram of the feature space

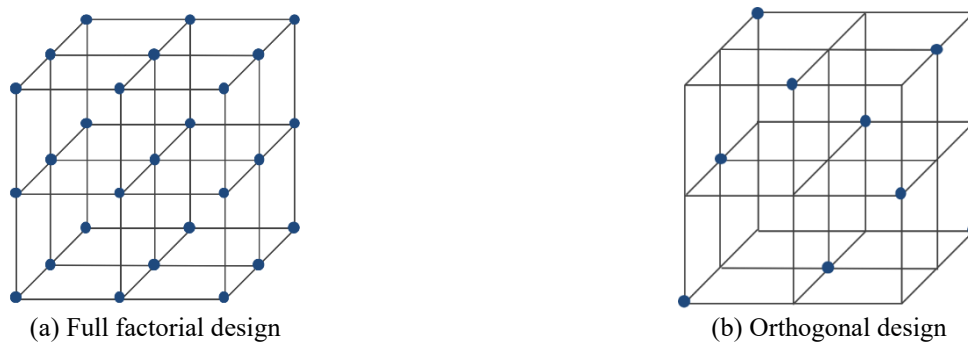


Fig. 3 Comparison of combinations for 3 factors and 3 levels per factor

samples) simulated from Monte Carlo simulation. More details of the proposed method are described in the following subsections.

## 2.2 Generation of the training samples

The step one starts with selecting main features affecting the tunnel face stability. In this study, six features are considered, including the tunnel diameter  $D$ , the cover depth  $H$ , the surcharge load  $\sigma$ , the unit weight  $\gamma$ , the cohesion  $c$ , and the friction angle  $\varphi$  of surrounding soils. In other words, an instance can be represented by a six-dimensional vector,  $\mathbf{x}_i = (D_i, H_i, \sigma_i, \gamma_i, c_i, \varphi_i)$ .

Then, an experimental domain is defined within the feature space. This is done by specifying the range of each factor. Consider, for example, a two-dimensional feature space of  $\gamma$  and  $D$ , the ranges of which can be specified as  $13 \leq x_1 \leq 24$  ( $\text{kN/m}^3$ ) and  $4 \leq x_2 \leq 15$  (m), respectively. For the convenience of visualization, Fig. 2 shows the subspace of  $\gamma$  and  $D$  bounded by the assigned ranges, which is defined as the experimental domain. The defined domain shall be large enough to cover most of routine cases in design practice. Instances that exceed this domain are deemed to be special cases which deserve special consideration. Within the specified domain, a set of combinations (denoted by  $\mathbf{x}_1, \mathbf{x}_2, \dots, \mathbf{x}_i$ ) of model parameters are determined, which are then labeled to form the training dataset. After this, a decision boundary is constructed. Unknown samples denoted by vectors can be

categorized as either stable (e.g.,  $\mathbf{x}_1^*$ ) or unstable (e.g.,  $\mathbf{x}_2^*$ ) samples according to the computed value of the decision function.

The commonly used experimental design methods include full factorial design, orthogonal design, and uniform design. Considering  $m$  factors and  $n$  levels per factor, full factorial design involves  $n^m$  combinations (experiments), which can be significantly decreased to  $n^2$  using an orthogonal design (Cavazzuti, 2013). Consider, for example,  $m = 6$  and  $n = 12$ , full factorial design will produce  $12^6 = 2985984$  samples. Labeling such a large number of training samples is computationally expensive. However, the orthogonal design only generates  $12^2 = 144$  combinations. Fig. 3 compares the combinations for 3 factors and 3 levels per factor produced by full factorial design and orthogonal design methods. Using the orthogonal design, the number of combinations is decreased from 27 to 9. However, the experimental domain is uniformly covered by selected combinations of model parameters, which are hence representative (Wang *et al.* 2013, Wang *et al.* 2014).

## 2.3 Labeling of the training samples

Finite element analyses are then utilized to label the training samples. This task is achieved using the strength reduction technique, by which the safety factor ( $F_s$ ) is calculated as:

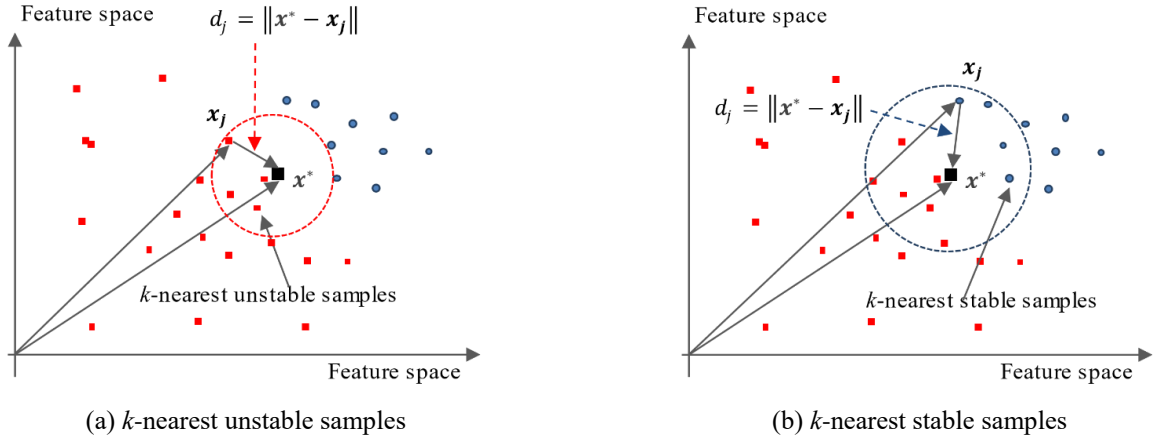
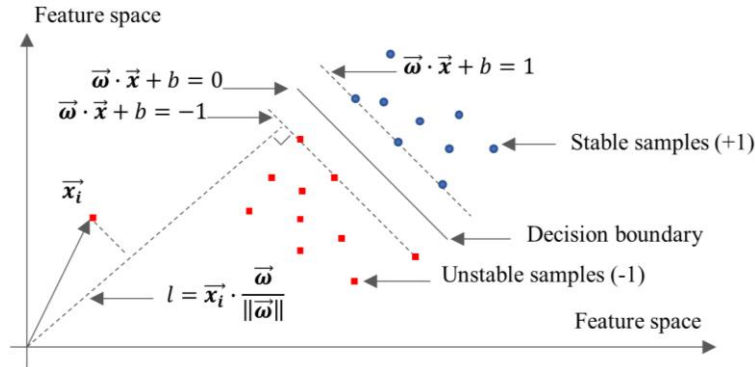


Fig. 4 Selection of instance-based training dataset

Fig. 5 The SVM classification algorithm (Duan *et al.* 2003)

$$F_s = \frac{c}{c_{cr}} = \frac{\tan \varphi}{\tan \varphi_{cr}} \quad (1)$$

where  $c$  and  $\varphi$  denote the strength parameters of surrounding soils;  $c_{cr}$  and  $\varphi_{cr}$  denote their critical values in terms of tunnel face stability. If  $F_s \geq 1$ , the tunnel face is stable; if  $F_s < 1$ , the tunnel face is unstable. Then, each instance,  $\mathbf{x}_i = (D_i, H_i, \sigma_i, \gamma_i, c_i, \varphi_i)$ , is labeled as stable ( $y_i = +1$ ) for  $F_s \geq 1$  or unstable ( $y_i = -1$ ), for  $F_s < 1$  to obtain a set of training samples:

$$\mathbf{D} = \{(\mathbf{x}_1, y_1), (\mathbf{x}_2, y_2), \dots, (\mathbf{x}_i, y_i)\} \quad (2)$$

#### 2.4 Selection of instance-based training samples

After the selected samples have been labeled, the training dataset  $\mathbf{D}$  is applied to performing classifications. For an unknown instance  $\mathbf{x}^*$ , the first step is to measure the distance between  $\mathbf{x}^*$  and each data point (represented by  $\mathbf{x}_j$ ) in the feature space. A commonly used distance can be defined by the Euclidean norm,  $d_j = \|\mathbf{x}^* - \mathbf{x}_j\|$ , as shown in Fig. 4. The measured distances are stored and sorted in an ascending order. The  $k$  data points that have the shortest distances from the unknown instance will be selected to form an instance-based training dataset  $\mathbf{D}^*$ . Considering the balance between the number of stable and unstable training samples, it is recommended to select  $k$  nearest unstable samples and  $k$  nearest stable samples,

respectively. In other words,  $2k$  samples will be selected to form  $\mathbf{D}^*$ .

#### 2.5 SVM-KNN classifiers

The instance-based training dataset  $\mathbf{D}^*$  is then used to train a SVM classifier. Fig. 5 illustrates the SVM algorithm (Duan *et al.* 2003). For the selected training samples, the aim is to determine a maximum-margin separating hyperplane, or named decision boundary that separates stable and unstable samples such that their distance is maximum.

The expression of the decision boundary may be written as (Goh and Goh 2007):

$$\bar{\omega} \cdot \bar{\mathbf{x}} + b = 0 \quad (3)$$

where  $\bar{\omega}$  represents the normal vector to the hyperplane;  $\bar{\mathbf{x}}$  represents the vector of a sample;  $b$  is a constant whose normalized form  $b/\|\bar{\omega}\|$  determines the offset of the hyperplane from the original along with the normal vector  $\bar{\omega}$ .

The maximum-margin hyperplane is taken as the optimal hyperplane for separating samples. In addition, there exist another two parallel hyperplanes which are expressed as:

$$\bar{\omega} \cdot \bar{\mathbf{x}}_i + b = 1, y_i = 1 \quad (4)$$

and

$$\vec{\omega} \cdot \vec{x}_i + b = -1, y_i = -1 \quad (5)$$

These  $\vec{x}_i$  are called support vectors that lie on the boundaries on both sides. The distance between these two hyperplanes is  $2/\|\vec{\omega}\|$ . The strategy is to maximize this distance, which is equivalent to minimize  $\|\vec{\omega}\|$ .

For all the stable samples, the constraint can be written as:

$$\vec{\omega} \cdot \vec{x}_i + b \geq 1, \text{ if } y_i = 1 \quad (6)$$

For the unstable samples, the constraint is written as:

$$\vec{\omega} \cdot \vec{x}_i + b \leq -1, \text{ if } y_i = -1 \quad (7)$$

The two constraints can be synthesized and be rewritten as:

$$y_i(\vec{\omega} \cdot \vec{x}_i + b) \geq 1, \text{ for all } 1 \leq i \leq n \quad (8)$$

The minimization of  $\|\vec{\omega}\|$  subject to the constraint given in Eq. (8) is known as a class of convex quadratic optimization problem. It can be solved by the method of Lagrange multipliers which introduces a set of variables called Lagrange multipliers (denoted by  $\alpha = (\alpha_1, \alpha_2, \dots, \alpha_m), \alpha_i \geq 0$ ) to define an auxiliary function:

$$L(\vec{\omega}, b, \alpha) = \frac{1}{2} \|\vec{\omega}\|^2 + \sum_{i=1}^m \alpha_i (1 - y_i(\vec{\omega} \cdot \vec{x}_i + b)) \quad (9)$$

and solve:

$$\frac{\partial L}{\partial \vec{\omega}} = 0; \quad \frac{\partial L}{\partial b} = 0 \quad (10)$$

The optimum of  $\vec{\omega}$  and  $b$  can be determined after the Lagrange multipliers have been solved based on Eqs. (9) and (10). Thereafter, the value of the decision function (Eq. (11)) of a new sample (denoted by  $\vec{x}_*$ ) can be computed as follows:

$$z = \text{sgn}(\vec{\omega} \cdot \vec{x}_* + b) \quad (11)$$

A positive value will assign the new sample to the stable category, while a negative value will assign it to the unstable category. Note that Eq. (11) represents a linear classifier, which is applicable to cases where the data is linearly separable. On the other hand, if the data is linearly inseparable, nonlinear classifiers can be developed by applying other kernels (Goh and Goh 2007, Samui 2008). Some common kernels include Polynomial (Eq. (12)), Gaussian radial basis function, RBF (Eq. (13)), and Sigmoid (Eq. (14)):

$$\kappa(\vec{x}_i, \vec{x}_j) = (\vec{x}_i \cdot \vec{x}_j)^d \quad (12)$$

$$\kappa(\vec{x}_i, \vec{x}_j) = \exp\left(-\gamma \|\vec{x}_i - \vec{x}_j\|^2\right) \quad (13)$$

$$\kappa(\vec{x}_i, \vec{x}_j) = \tanh(\kappa \vec{x}_i \cdot \vec{x}_j + c) \quad (14)$$

where  $\vec{x}_i$  and  $\vec{x}_j$  denote vectors in the feature space,  $d$  and  $c$  are constants,  $\gamma$  denotes the variance of Gaussian kernel. By incorporating one kernel into the decision function, a new sample can be classified by computing:

$$z = \text{sgn}(\vec{\omega} \cdot \varphi(\vec{z}) - b) = \text{sgn}\left(\left[\sum_{i=1}^n c_i y_i k(\vec{x}_i, \vec{z})\right] - b\right) \quad (15)$$

where  $\vec{z}$  denotes the vector of the new sample;  $\vec{x}_i$  denotes the support vectors which depend on the used kernel and the training samples,  $c_i$  denote coefficients,  $b$  is a constant. Before the classifier is applied to classifying new samples, validation is needed to examine its prediction accuracy. A commonly used indicator is the average accuracy:

$$\text{Average accuracy} = \frac{n_T}{n_F + n_T} \quad (16)$$

where  $n_F$  and  $n_T$  represent the number of false and true classifications, respectively. Note that the prediction accuracy on both training and test datasets have to be checked. A test dataset refers to a dataset that is different from the training dataset. It can be obtained either by collecting some new samples that are not included in the training dataset or by employing the  $k$ -fold cross-validation technique. The  $k$ -fold cross-validation method splits the training dataset into  $k$  subsets, each of which is held as testing dataset to check the prediction accuracy of the classifier trained from the remaining subsets.

### 3. Illustrative examples

#### 3.1 Training of SVM classifiers

In this section, deterministic and probabilistic application examples are presented to illustrate the proposed method. Consider, for example, the six impact factors shown in Table 1. Their values are specified within certain ranges so as to cover routine cases in practice. Each feature is assigned to has 12 levels within these ranges. For cases that exceed the specified domain, it is recommended to perform specific studies case by case. If it is necessary, both the ranges and levels of the six features considered in this example can be modified deemed appropriate to meet particular requirements. After the experimental domain and the level of each factor have been determined, the orthogonal design is utilized to produce 144 samples, each of which is labeled by the two-dimensional finite element analysis.

It should be emphasized that tunnel face stability is more appropriate to be simulated by three-dimensional modeling. However, it requires great effort to build 144 different 3D numerical models, and huge computational costs to complete 144 3D numerical simulations as well. Since the main purpose here is to validate the feasibility and efficiency of the proposed method, this example utilizes 2D simulations to label the samples. Moreover, the main concern is not the values of the safety factors, but the labels that depend on if the safety factors are larger than 1.0. This means that the labels of most samples are reliable even though they are determined based on 2D simulation results. Only a few samples that are close to the limit state may have different labels due to the simplification in 2D modeling in comparison with 3D modeling (Li and Li 2019).

Table 1 Six impact factors and twelve levels per factor

Factors/Levels	$D/m$	$H/m$	$\sigma_s/kPa$	$\gamma(kN/m^3)$	$c/kPa$	$\varphi/^\circ$
1	4	5	0	13	0	0
2	5	10	10	14	4	4
3	6	15	20	15	8	8
4	7	20	30	16	12	12
5	8	25	40	17	16	16
6	9	30	50	18	20	20
7	10	35	60	19	24	24
8	11	40	70	20	28	28
9	12	45	80	21	32	32
10	13	50	90	22	36	36
11	14	55	100	23	40	40
12	15	60	110	24	44	44

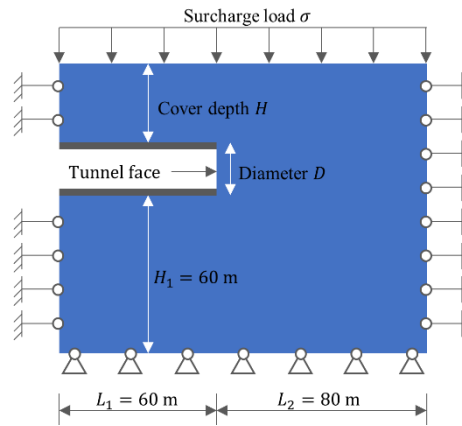


Fig. 6 Schematic diagram of the numerical model and boundary conditions

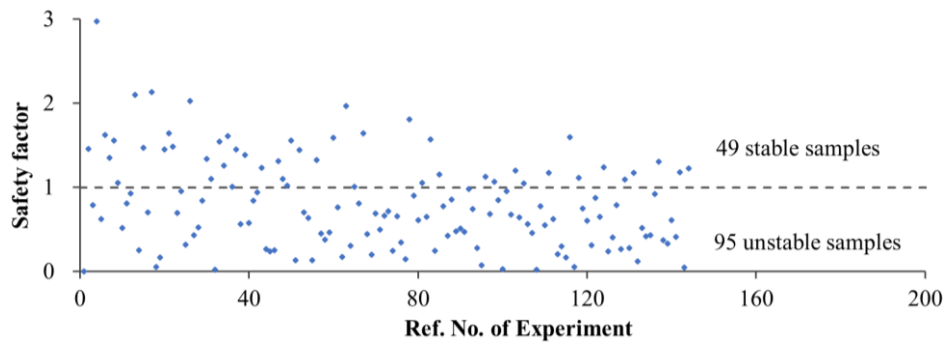


Fig. 7 Safety factors of the training samples

The software OptumG2 was used for numerical simulations. Fig. 6 shows the schematic diagram of a two-dimensional finite element model, in which the geometry parameters and boundary conditions are indicated. For a 2D numerical model, the vertical (left and right) boundaries can be constrained either in the horizontal direction, or in both the horizontal and vertical directions. Existing studies (e.g., Mollon *et al.* 2011) showed that the two setting-ups provide the same results, indicating that only using horizontal constrain is sufficient. For 3D numerical models, the left and right boundaries are usually constrained in the

horizontal direction while the bottom boundary is constrained in both the horizontal and vertical directions. The boundary conditions used in this paper are consistent with those adopted for 3D numerical models that are commonly-used in the literature (e.g., Mollon *et al.* 2009b, Paternesi *et al.* 2017, Pan and Dias, 2018). Some other geometry parameters ( $H_1$ ,  $L_1$  and  $L_2$ ) are constant, values of which were chosen so as not to affect the tunnel face stability (avoid boundary effects).

The soil is modeled as an elasto-plastic material following Mohr-Coulomb failure criterion. The mesh is

Table 2 Average accuracies of different classifiers

Kernel functions	Average accuracy	
	SVM-KNN	SVM
Linear	0.972	0.958
Polynomial (degree = 2)	1.000	1.000
Polynomial (degree = 3)	1.000	1.000
RBF	0.993	1.000
Sigmoid	0.683	0.660

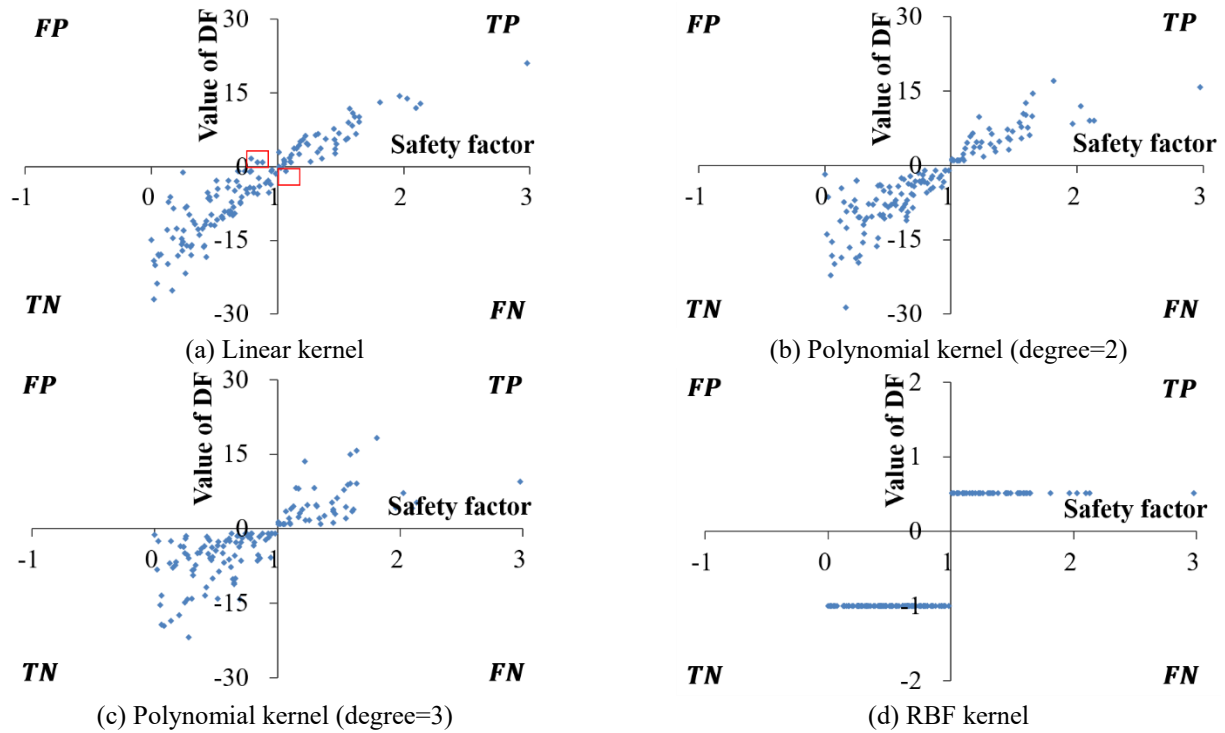


Fig. 8 Safety factor versus value of decision function

assigned to 2000 adaptive elements. The built-in strength reduction analysis was employed to compute the safety factors of the training samples, among which there are 95 unstable samples and 49 stable samples, as shown Fig. 7. Thereafter, the step one of the proposed approach is completed and the total training data  $\mathbf{D}$  is obtained.

Step two starts with determining an instance-based training dataset  $\mathbf{D}^*$ , followed by training an instance-based SVM classifier. In this example, the value of  $k$  is set to its maximum, 49, as it is the number of stable samples in the complete training dataset. As a result, for each unknown instance, all the stable samples and 49 nearest unstable samples will be selected to form  $\mathbf{D}^*$ . This procedure is implemented with an ad hoc Python program, which also imports the SVM modulus from scikit-learn to fit the training data  $\mathbf{D}^*$ . Kernel functions including Linear kernel, Polynomial kernel, Gaussian kernel (RBF), and Sigmoid kernel are employed to construct both linear and nonlinear SVM-KNN classifiers.

For comparison, the complete training dataset  $\mathbf{D}$  is also used to construct several SVM classifiers with different kernel functions. The average accuracies of these classifiers

are shown in Table 2. Generally, combining SVM with KNN slightly improves the prediction accuracies on the training data. The performance of the classifier with the sigmoid kernel function is the worst as indicated by its lowest prediction accuracy on the training data (Van *et al.* 2010). It is therefore not suitable for separating new samples.

The prediction performance of the SVM classifiers can be observed according to the relationship between the simulated safety factors (denoted as FS) and the computed values of decision functions (denoted as DF), as shown in Fig 8. The points that lie in the first and third quadrants represent true positive (TP) and negative (TN) samples, respectively. In contrast, the points that lie in the second and fourth quadrants represent false positive and negative samples, respectively, which are misclassified samples as indicated by red rectangles. The comparison between Fig. 8(a) and 8(b) demonstrates that the polynomial kernel function can give better prediction than the linear kernel function for samples that are very close to the limit state (DF=0, FS=1).

Although the above classifiers are not underfitting, it

Table 3 Results of  $k$ -fold cross-validation ( $k = 10$ )

Kernel functions	Average accuracy	
	SVM-KNN	SVM
Linear	0.959	0.945
Polynomial (degree = 2)	0.945	0.924
Polynomial (degree = 3)	0.938	0.966
RBF	0.683	0.660

Table 4 Evaluations of tunnel face stability with existing samples

$D$	$H$	$\sigma$	$\gamma$	$c$	$\varphi$	Mollon (2010) ( $\sigma_c$ )	Chambon (1994)( $\sigma_c$ )	SVM-KNN	SVM	$F_s$
5	2.5	0	16.1	0	38	6.8	3.6	-2.44	-4.07	0.186
5	2.5	0	16.1	5	38	0.4	3.6	-1.55	-2.45	0.776
5	2.5	0	16.1	0	42	5.3	3.6	-2.80	-4.67	0.215
5	2.5	0	16.1	5	42	Stable	3.6	-1.81	-2.87	0.776
5	2.5	0	15.3	0	38	6.5	4.2	-2.44	-4.09	0.186
5	2.5	0	15.3	5	38	0.1	4.2	-1.55	-2.48	0.801
5	2.5	0	15.3	0	42	5	4.2	-2.81	-4.70	0.215
5	2.5	0	15.3	5	42	Stable	4.2	-1.82	-2.90	0.856
10	10	0	16	0	38	13.6	7.4	-3.20	-5.23	0.155
10	10	0	16	5	38	7.1	7.4	-2.32	-3.71	0.547
10	10	0	16	0	42	10.5	7.4	-3.52	-5.77	0.179
10	10	0	16	5	42	5	7.4	-2.54	-4.07	0.598
13	42	0	16.2	0	38	17.9	13	-3.10	-4.98	0.154
13	42	0	16.2	5	38	11.4	13	-2.08	-3.35	0.487
13	42	0	16.2	0	42	13.8	13	-3.00	-4.92	0.177
13	42	0	16.2	5	42	8.3	13	-1.88	-3.11	0.518

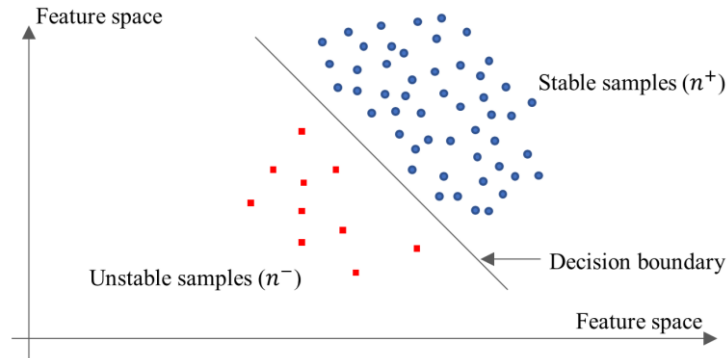


Fig. 9 Illustration of probabilistic applications

still needs to examine their performance on test data to avoid overfitting. This study employs a 10-fold cross-validation to perform this task. For this purpose, the training data was divided into 10 subsets, each of which was held as testing data to check the prediction accuracy of the classifier trained by the remaining 9 subsets. The average accuracy of SVM-KNN and SVM classifiers on testing data are presented in Table 3.

The classifiers that are constructed based on the RBF have low prediction accuracies on testing data, which means that they are deemed to be overfitting. On the contrary, other classifiers that have relatively high

prediction accuracies can be therefore used to classify unknown samples in the following analysis. During this validation process, the use of KNN also slightly improved the prediction accuracies of the classifiers using the linear, polynomial (degree = 2) and RBF kernel functions.

### 3.2 Deterministic application example

This section presents results of deterministic applications. Table 4 listed some experimental and computed collapse pressures in the existing literature (Chambon and Corte 1994, Mollon *et al.* 2010), where the

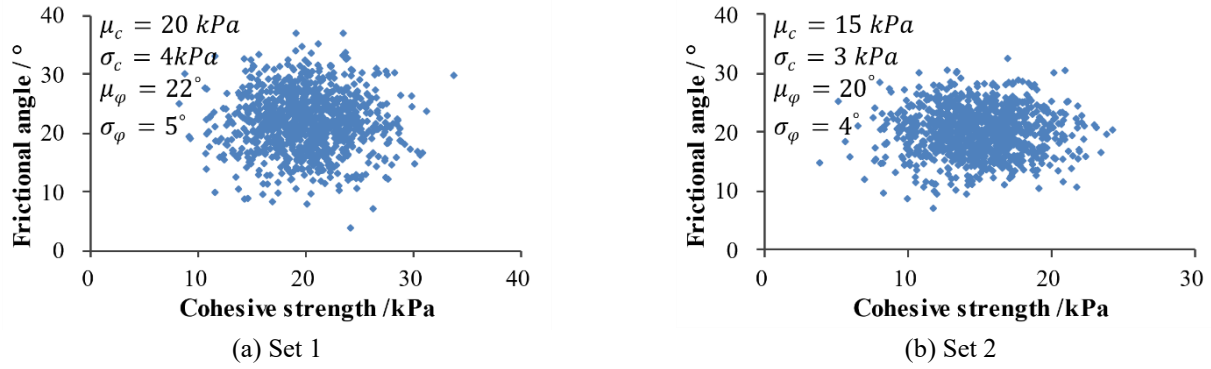
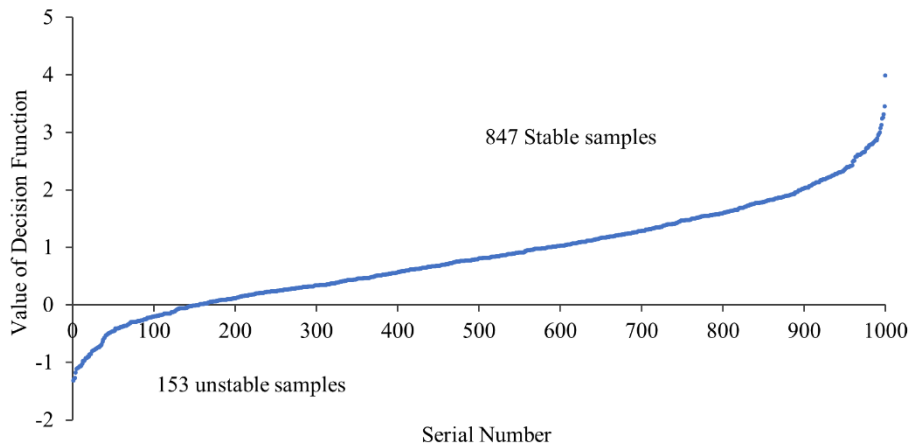

 Fig. 10 Two set of statistics of  $c$  and  $\varphi$  and their corresponding samples


Fig. 11 Calculation of the failure probability

Table 5 Simulated safety factors and reliability indexes

Dataset	Set 1			Set 2		
	$c/kPa$	$\varphi/^\circ$	$F_s$	$c/kPa$	$\varphi/^\circ$	$F_s$
Point 1	20	22	1.223	15	20	1.011
Point 2	24	22	1.327	15	24	1.127
Point 3	16	22	1.101	15	16	0.888
Point 4	20	27	1.383	18	20	1.099
Point 5	20	17	1.052	12	20	0.913
<b>Reliability index, <math>\beta</math></b>		1.075			0.073	

computed values of the decision functions (based on polynomial with degree = 2) are included as well as the simulated safety factors.

The variable  $\sigma_c$  represents the limit pressure that is required to be applied on the tunnel face to avoid face collapse. Almost all the presented cases have positive values of  $\sigma_c$ , indicating that the tunnel faces are initially unstable. The two cases with no collapse pressure (Mollon *et al.* 2010) means that the tunnel faces are initially stable. These states can be alternatively evaluated using the SVM-KNN and SVM classifiers. All the computed values of the decision function are negative, classifying all these cases into the unstable category. On the other hand, results are validated according to numerical calculations, in which all the simulated safety factors are less than 1.0.

### 3.3 Probabilistic application example

Probabilistic evaluations may be performed by Monte Carlo simulations based on deterministic models (Cao *et al.* 2017). As illustrated in Fig. 9, a number of Monte Carlo samples can be first simulated from prescribed distributions of uncertain parameters (e.g., uncertain features concerned in design), and each Monte Carlo sample is then used as input in deterministic models (e.g., SVM-KNN classifiers in this study) to obtain its corresponding predictions (e.g., stable or unstable).

Let  $n^-$  and  $n^+$  be the number of unstable and stable predictions, respectively. The failure probability of the tunnel face is calculated as:

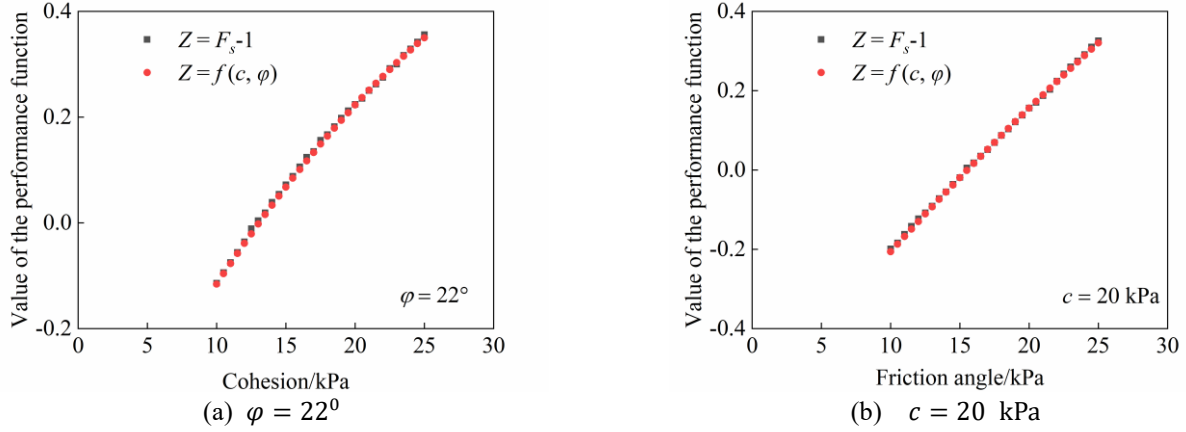


Fig. 12 Comparison of the values of the performance function

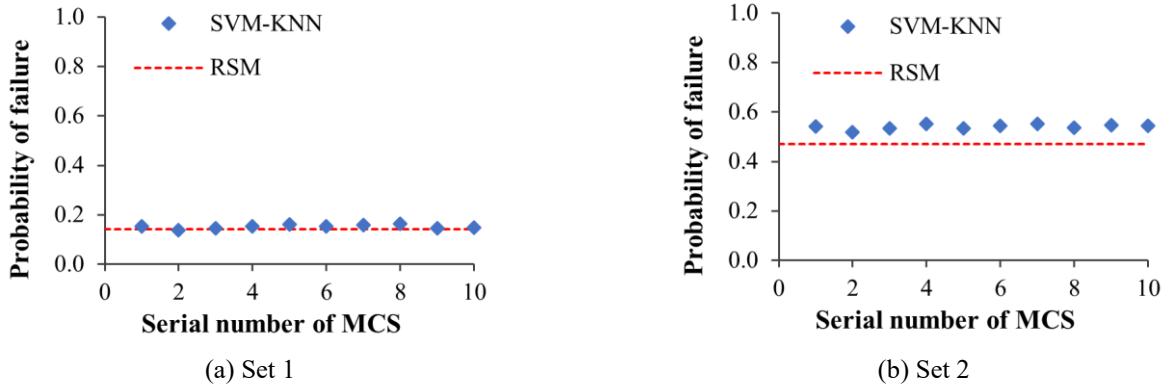


Fig. 13 Failure probabilities determined by RSM and SVM-KNN (10 times MCS)

$$p_f = \frac{n^-}{n^- + n^+} \quad (17)$$

Generating Monte Carlo samples and calculating the failure probability is also performed by an in-house Python program in this study. For instance, consider a tunnel example with the vector of parameters  $\mathbf{x} = [4, 20, 0, 19, c, \varphi]$ , in which  $c$  and  $\varphi$  are assumed to be normal random variables. The probability density functions of  $c$  and  $\varphi$  can be given as follows:

$$f_c = \frac{1}{\sqrt{2\pi} \cdot \sigma_c} e^{\left(\frac{-(c-\mu_c)^2}{2\sigma_c^2}\right)} \quad (18)$$

$$f_\varphi = \frac{1}{\sqrt{2\pi} \cdot \sigma_\varphi} e^{\left(\frac{-(\varphi-\mu_\varphi)^2}{2\sigma_\varphi^2}\right)} \quad (19)$$

where  $\mu_c$  and  $\sigma_c$  denote the mean and standard deviation of the cohesive strength, respectively;  $\mu_\varphi$  and  $\sigma_\varphi$  denote the mean and standard deviation of the frictional angle, respectively. Fig. 10 shows the two sets of statistics of  $c$  and  $\varphi$ , and their corresponding samples generated from Monte Carlo simulations.

For the first set of samples, the values of decision function with polynomial kernel function (degree = 2) were calculated and sorted in an ascending order. As shown

in Fig. 11, 153 out of 1000 samples were predicted to be unstable. Hence, the failure probability of the tunnel face is 15.3%.

For validation, the failure probabilities of the two cases are also computed using the Response Surface Method. According to the existing studies, the performance function concerning tunnel face stability can be represented by a quadratic polynomial equation (Mollon *et al.* 2009b, Li and Yang, 2018, Hamrouni *et al.* 2019):

$$Z = F_s - 1 = a_0 + a_1c + a_2\varphi + a_3c^2 + a_4\varphi^2 \quad (20)$$

where  $a_0$  and  $a_i$  denote the unknown coefficients. For each case, the central composite design (CCD) is used to sample five points. The performance function is solved with the safety factors of the five points simulated in strength reduction analyses, enabling the reliability indexes of the two cases to be computed using the Advanced First-Order Second-Moment method, as shown in Table 5.

To validate the accuracy of the performance function, two sets of datapoints are adopted to conduct strength reduction analyses. The first set of datapoints have a constant value of the friction angle ( $\varphi = 22^\circ$ ) while the second set of datapoints have a constant value of the cohesion ( $c = 20$  kPa). In addition, Eq. (20) is adopted to calculate the values of the performance function of these datapoints. Fig. 12 compares the values of the performance function calculated using the simulated safety factors to

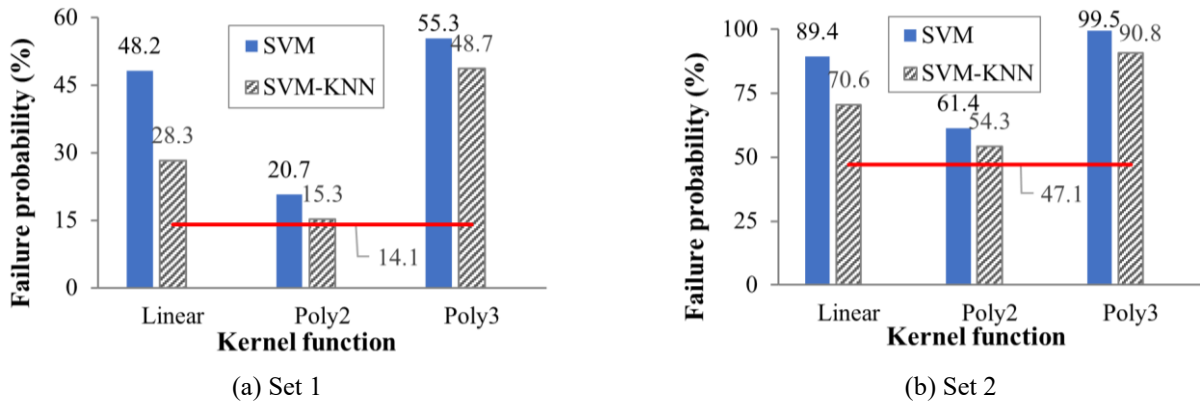


Fig. 14 Comparison of failure probabilities

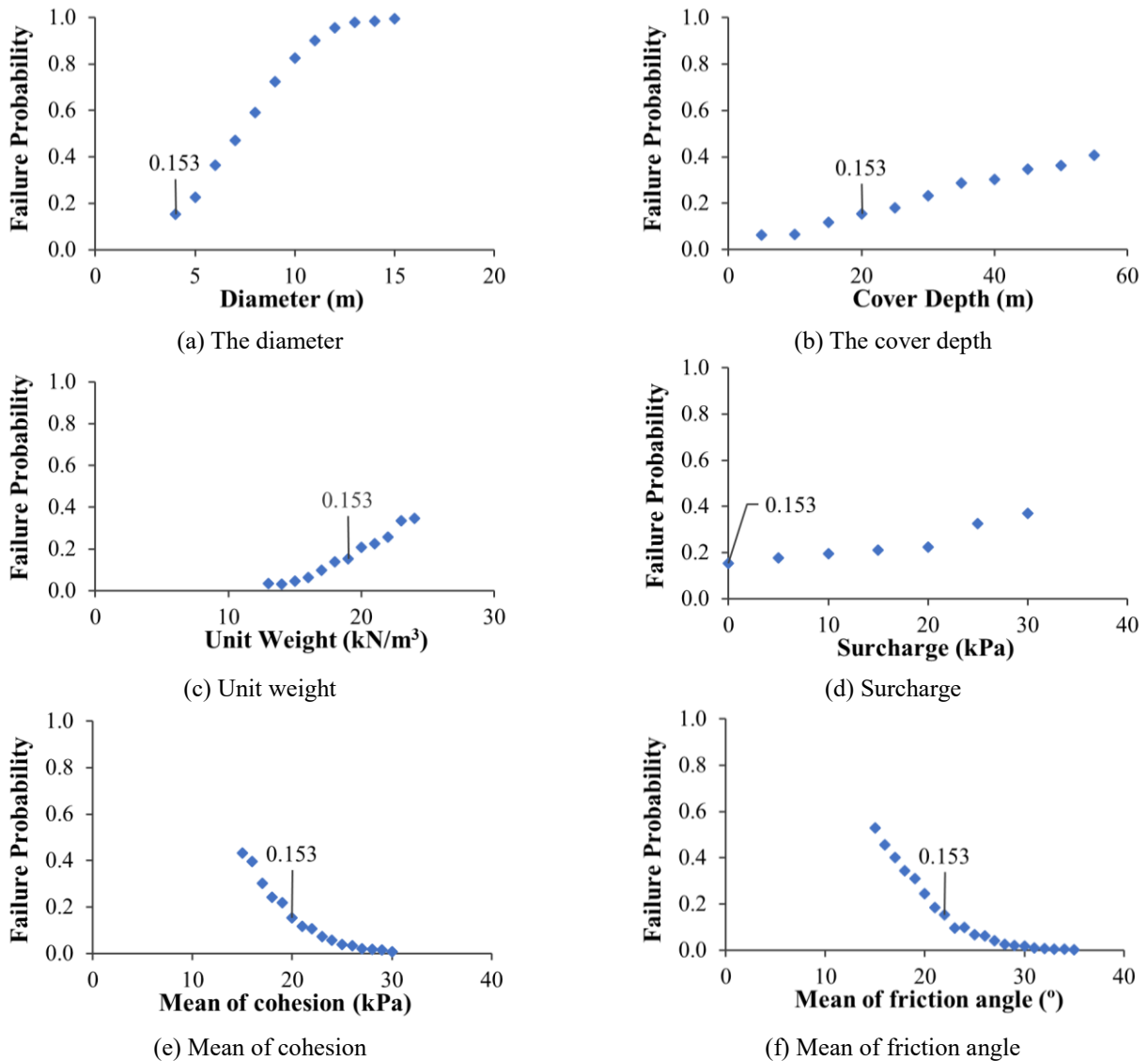


Fig. 15 Influence of factors on failure probability

those calculated using Eq. (20). Results demonstrate that RSM can give an accurate approximation of the performance function concerning tunnel face stability.

Based on Eq. (21), the failure probabilities of the two cases are determined to be 14.1% and 47.1%, respectively.

$$p_f = 1 - \Phi(\beta) \quad (21)$$

where  $\Phi$  represents the standard normal cumulative distribution function (CDF).

In the SVM-KNN method, Monte Carlo samples are

randomly generated, the failure probability may vary from one run to another due to random fluctuation. Fig. 13 shows the computed failure probabilities obtained by 10 runs of Monte Carlo simulations, yielding 10 estimates of failure probabilities. The mean values of these 10 failure probabilities is 15.2% and 54.0%, respectively. Generally, these results compare well with those determined by RSM, which validates the proposed method.

Fig. 14 compares the performance in probabilistic applications between SVM-KNN and SVM classifiers constructed based on different kernel functions, where the failure probabilities calculated using RSM are represented by red solid lines. Results show that SVM-KNN classifiers can give better estimations of the failure probabilities than SVM classifiers. On the other hand, the polynomial kernel function with degree = 2 is found to be the most suitable kernel function in probabilistic applications.

In fact, the accuracy of the failure probability relies on the similarity between the trained decision function and the real limit state function. The SVM uses only one decision function to separate all input samples, whereas SVM-KNN utilizes a instance-dependent localized decision function for each sample. The instance-based classifier has a better performance in classification since it makes use a localized decision boundary. This is why SVM-KNN gives more accurate estimations of failure probabilities.

Moreover, the procedures of the proposed approach (including generation of Monte Carlo samples, selection of instance-based training dataset, construction of instance-based classifiers, classification of Monte Carlo samples, as well as the calculation of failure probability) can be completed within several seconds. Whereas RSM requires five numerical simulations for each case specified by geometric parameters (e.g.,  $H$ ,  $D$ ) to obtain the safety factors to develop the instance-based performance function. Such a process is relatively easy for a single case with specific geometric parameters but very time-consuming and tedious for a number of cases if geometric parameters can vary, which is of great interest in design practice.

To show the convenience and efficiency of the proposed method, six groups of failure probabilities are estimated. For each group of calculations, only one factor varies in an interval to re-evaluate the corresponding failure probability of the tunnel face while the other factors remain constant. The failure probability of each case was computed with ignorable computational costs. By this means, the relationship between each factor and the failure probability is obtained, as shown in Fig. 15, where the failure probability ( $p_f = 0.153$ ) of the original case is also indicated.

Generally, the failure probability increases with the increase of the diameter, the cover depth, the unit weight, and the surcharge, but decreases with the increase of the cohesion and the friction angle, which are consistent with intuitive experience in design practice.

#### 4. Conclusions

This paper proposed an efficient method to facilitate deterministic and probabilistic evaluations of tunnel face

stability according to binary classifications. In the illustrative examples, the procedures of proposed approach are performed in an ad hoc python program. By this means, both deterministic and probabilistic evaluations of tunnel face stability can be automatically completed within negligible computational efforts. Based on this study, several major conclusions can be drawn:

- Applicability of the classifiers can be improved by expanding the ranges deemed appropriate, whereas the performance of the classifiers can be improved by collecting more training samples. SVM-KNN gives relatively accurate results, particularly in probabilistic evaluations because it trains a localized decision function for each sample, whereas SVM separates all the samples using a single decision function.

- Another crucial influence on the performance of a classifier is the kernel function. The polynomial kernel function with degree = 2 is found to be the most suitable one to train nonlinear classifiers with relatively high performance for tunnel face stability analysis in this study. Selection of the kernel function in probabilistic evaluations is much more important than in deterministic evaluations. This is mainly because there might be many instances located close to the decision function. These instances are sensitive to the change in the position of the decision function.

- Both deterministic and probabilistic evaluations can be completed within several seconds, allowing a number of evaluations to be performed in a cost-effective manner. The convenience and efficiency of the proposed method make it very useful in design practice, particularly when real-time evaluations are required, because the factors (including geometric parameters) that influence tunnel face stability may vary from one location to another along the tunnel.

#### Acknowledgments

This study is supported by the National Natural Science Foundation of China (No.51608407), the NRF-NSFC 3rd Joint Research Grant (Earth Science) (No. 41861144022), the Fundamental Research Funds for the Central Universities (No. 2042019kf1022), and the China Scholarship Council (No. 201706955065).

#### References

- Anagnostou, G. and Perazzelli, P. (2013), "The stability of a tunnel face with a free span and a non-uniform support", *Geotechnik*, **36**(1), 40-50. <https://doi.org/10.1002/gete.201200014>.
- Bourinet, J.M., Deheeger, F. and Lemaire, M. (2011), "Assessing small failure probabilities by combined subset simulation and Support Vector Machines", *Struct. Saf.*, **33**(6), 343-353. <https://doi.org/10.1016/j.strusafe.2011.06.001>.
- Cao, Z., Wang, Y. and Li, D. (2017), *Probabilistic Approaches for Geotechnical Site Characterization and Slope Stability Analysis*, Springer, Berlin, Germany.
- Cavazzuti, M. (2013), *Optimization Methods*. Springer, Berlin, Germany.
- Chambon, P. and Corte, J.F. (1994), "Shallow tunnels in cohesionless soil: stability of tunnel face", *J. Geotech. Eng.*,

- 120(7), 1148-1165.  
[https://doi.org/10.1061/\(ASCE\)0733-9410\(1994\)120:7\(1148\)](https://doi.org/10.1061/(ASCE)0733-9410(1994)120:7(1148)).
- Chan, H.P., Sahiner, B. and Hadjiiski, L. (2004), "Sample size and validation issues on the development of CAD systems", *Int. Congr. Ser.*, **1268**, 872-877.  
<https://doi.org/10.1016/j.ics.2004.03.226>.
- Dias, D. (2011), "Convergence-confinement approach for designing tunnel face reinforcement by horizontal bolting", *Tunn. Undergr. Sp. Tech.*, **26**(4), 517-523.  
<https://doi.org/10.1016/j.tust.2011.03.004>.
- Duan, K., Keerthi, S.S. and Poo, A.N. (2003), "Evaluation of simple performance measures for tuning SVM hyperparameters", *Neurocomputing*, **51**, 41-59.  
[https://doi.org/10.1016/S0925-2312\(02\)00601-X](https://doi.org/10.1016/S0925-2312(02)00601-X).
- Goh, A.T.C. and Goh, S.H. (2007), "Support vector machines: Their use in geotechnical engineering as illustrated using seismic liquefaction data", *Comput. Geotech.*, **34**(5), 410-421.  
<https://doi.org/10.1016/j.compgeo.2007.06.001>.
- Hamrouni, A., Dias, D. and Sbartai, B. (2019), "Probability analysis of shallow circular tunnels in homogeneous soil using the surface response methodology optimized by a genetic algorithm", *Tunn. Undergr. Sp. Tech.*, **86**, 22-33.  
<https://doi.org/10.1016/j.tust.2019.01.008>.
- ITA/AITES (2007), "Settlements induced by tunnelling in soft ground", *Tunn. Undergr. Sp. Tech.*, **22**(2), 119-149.  
<https://doi.org/10.1016/j.tust.2006.11.001>.
- Juneja, A., Hegde, A., Lee, F.H. and Yeo, C.H. (2010), "Centrifuge modelling of tunnel face reinforcement using forepoling", *Tunn. Undergr. Sp. Tech.*, **25**(4), 377-381.  
<https://doi.org/10.1016/j.tust.2010.01.013>.
- Kamata, H. and Mashimo, H. (2003), "Centrifuge model test of tunnel face reinforcement by bolting", *Tunn. Undergr. Sp. Tech.*, **18**(2-3), 205-212.  
[https://doi.org/10.1016/S0886-7798\(03\)00029-4](https://doi.org/10.1016/S0886-7798(03)00029-4).
- Khezri, N., Mohamad, H. and Fatahi, B. (2016), "Stability assessment of tunnel face in a layered soil using upper bound theorem of limit analysis", *Geomech Eng.*, **11**(4), 471-492.  
<https://doi.org/10.12989/gae.2016.11.4.471>.
- Klar, A., Osman, A.S. and Bolton, M. (2007), "2D and 3D upper bound solutions for tunnel excavation using 'elastic' flow fields", *Int. J. Numer. Anal. Met.*, **31**(12), 1367-1374.  
<https://doi.org/10.1002/nag.597>.
- Leca, E. and Dormieux, L. (1990), "Upper and lower bound solutions for the face stability of shallow circular tunnels in frictional material", *Geotechnique*, **40**(4), 581-606.  
<https://doi.org/10.1680/geot.1990.40.4.581>.
- Lee, Y.J. (2016), "Determination of tunnel support pressure under the pile tip using upper and lower bounds with a superimposed approach", *Geomech. Eng.*, **11**(4), 587-605.  
<https://doi.org/10.12989/gae.2016.11.4.587>.
- Li, B. and Li, H. (2019), "Prediction of tunnel face stability using a naive bayes classifier", *Appl. Sci.*, **9**(19), 4139.  
<https://doi.org/10.3390/app9194139>.
- Li, B., Hong, Y., Gao, B., Qi, T.Y., Wang, Z.Z. and Zhou, J.M. (2015), "Numerical parametric study on stability and deformation of tunnel face reinforced with face bolts", *Tunn. Undergr. Sp. Tech.*, **47**, 73-80.  
<https://doi.org/10.1016/j.tust.2014.11.008>.
- Li, T.Z. and Yang, X.L. (2019a), "Probabilistic analysis for face stability of tunnels in Hoek-Brown media", *Geomech. Eng.*, **18**(6), 595-603. <https://doi.org/10.12989/gae.2019.18.6.595>.
- Li, T.Z. and Yang, X.L. (2019b), "Face stability analysis of rock tunnels under water table using Hoek-Brown failure criterion", *Geomech. Eng.*, **18**(3), 235-245.  
<https://doi.org/10.12989/gae.2019.18.3.235>.
- Li, T.Z. and Yang, X.L. (2019c), "An efficient uniform design for Kriging-based response surface method and its application", *Comput. Geotech.*, **109**, 12-22.  
<https://doi.org/10.1016/j.compgeo.2019.01.009>.
- Li, T.Z. and Yang, X.L. (2018), "Reliability analysis of tunnel face in broken soft rocks using improved response surface method", *Int. J. Geomech.*, **18**(5), 04018021.  
[https://doi.org/10.1061/\(ASCE\)GM.1943-5622.0001129](https://doi.org/10.1061/(ASCE)GM.1943-5622.0001129).
- Li, X., Li, X.B. and Su, Y.H. (2016), "A hybrid approach combining uniform design and support vector machine to probabilistic tunnel stability assessment", *Struct. Saf.*, **61**, 22-42. <https://doi.org/10.1016/j.strusafe.2016.03.001>.
- Mahdevari, S., Torabi, S.R. and Monjezi, M. (2012), "Application of artificial intelligence algorithms in predicting tunnel convergence to avoid TBM jamming phenomenon", *Int. J. Rock Mech. Min. Sci.*, **55**, 33-44.  
<https://doi.org/10.1016/j.ijrmm.2012.06.005>.
- Mollon, G., Dias, D. and Soubra, A.H. (2011), "Rotational failure mechanisms for the face stability analysis of tunnels driven by a pressurized shield", *Int. J. Numer. Anal. Meth. Geomech.*, **35**(12), 1363-1388. <https://doi.org/10.1002/nag.962>.
- Mollon, G., Phoon, K.K., Dias, D. and Soubra, A.H. (2011), "Validation of a new 2D failure mechanism for the stability analysis of a pressurized tunnel face in a spatially varying sand", *J. Eng. Mech.*, **137**(1), 8-21.  
[https://doi.org/10.1061/\(ASCE\)EM.1943-7889.0000196](https://doi.org/10.1061/(ASCE)EM.1943-7889.0000196).
- Mollon, G., Dias, D. and Soubra, A.H. (2010), "Face stability analysis of circular tunnels driven by a pressurized shield", *J. Geotech. Geoenviron. Eng.*, **136**(1), 215-229.  
[https://doi.org/10.1061/\(ASCE\)GT.1943-5606.0000194](https://doi.org/10.1061/(ASCE)GT.1943-5606.0000194).
- Mollon, G., Dias, D. and Soubra, A.H. (2009a), "Probabilistic analysis and design of circular tunnels against face stability", *Int. J. Geomech.*, **9**(6), 237-249.  
[https://doi.org/10.1061/\(ASCE\)1532-3641\(2009\)9:6\(237\)](https://doi.org/10.1061/(ASCE)1532-3641(2009)9:6(237)).
- Mollon, G., Dias, D. and Soubra, A.H. (2009b), "Probabilistic analysis of circular tunnels in homogeneous soil using response surface methodology", *J. Geotech. Geoenviron. Eng.*, **135**(9), 1314-1325.  
[https://doi.org/10.1061/\(ASCE\)GT.1943-5606.0000060](https://doi.org/10.1061/(ASCE)GT.1943-5606.0000060).
- Ng, C.W.W. and Lee, G.T.K. (2002), "A three-dimensional parametric study of the use of soil nails for stabilising tunnel faces", *Comput. Geotech.*, **29**(8), 673-697.  
[https://doi.org/10.1016/S0266-352X\(02\)00012-5](https://doi.org/10.1016/S0266-352X(02)00012-5).
- Pal, M. (2006), "Support vector machines-based modelling of seismic liquefaction potential", *Int. J. Numer. Anal. Met.*, **30**(10), 983-996. <https://doi.org/10.1002/nag.509>.
- Pan, Q. and Dias, D. (2018), "Three dimensional face stability of a tunnel in weak rock masses subjected to seepage forces", *Tunn. Undergr. Sp. Tech.*, **71**, 555-566.  
<https://doi.org/10.1016/j.tust.2017.11.003>.
- Pan, Q. and Dias, D. (2017), "An efficient reliability method combining adaptive Support Vector Machine and Monte Carlo Simulation", *Struct. Saf.*, **67**, 85-95.  
<https://doi.org/10.1016/j.strusafe.2017.04.006>.
- Patemesi, A., Schweiger, H.F. and Scarpelli, G. (2017), "Numerical analyses of stability and deformation behavior of reinforced and unreinforced tunnel faces", *Comput. Geotech.*, **88**, 256-266. <https://doi.org/10.1016/j.compgeo.2017.04.002>.
- Pham, B.T., Bui, D.T., Dholakia, M.B., Prakash, I. and Pham, H.V. (2016), "A comparative study of least square support vector machines and multiclass alternating decision trees for spatial prediction of rainfall-induced landslides in a tropical cyclones area", *Geotech. Geol. Eng.*, **34**(6), 1807-1824.  
<https://doi.org/10.1007/s10706-016-9990-0>.
- Qiu, Z., Ruan, J., Huang, D., Wei, M., Tang, L., Huang, C., Xu, W. and Shu, S. (2016), "Hybrid prediction of the power frequency breakdown voltage of short air gaps based on orthogonal design and support vector machine", *IEEE T. Dielectr. Electr. Insul.*, **23**(2), 795-805. <https://doi.org/10.1109/TDEI.2015.005398>.

- Samui, P. (2008), "Support vector machine applied to settlement of shallow foundations on cohesionless soils", *Comput. Geotech.*, **35**(3), 419-427. <https://doi.org/10.1016/j.compgeo.2007.06.014>.
- Samui, P. and Karthikeyan, J. (2013), "Determination of liquefaction susceptibility of soil: A least square support vector machine approach", *Int. J. Numer. Anal. Met.*, **37**(9), 1154-1161. <https://doi.org/10.1002/nag.2081>.
- Shi, S., Zhao, R., Li, S., Xie, X., Li, L., Zhou, Z. and Liu, H. (2019), "Intelligent prediction of surrounding rock deformation of shallow buried highway tunnel and its engineering application", *Tunn. Undergr. Sp. Tech.*, **90**, 1-11. <https://doi.org/10.1016/j.tust.2019.04.013>.
- Tinoco, J., Correia, A.G. and Cortez, P. (2014), "Support vector machines applied to uniaxial compressive strength prediction of jet grouting columns", *Comput. Geotech.*, **55**, 132-140. <https://doi.org/10.1016/j.compgeo.2013.08.010>.
- Van der Aalst, W.M., Rubin, V., Verbeek, H.M.W., van Dongen, B.F., Kindler, E. and Günther, C.W. (2010), "Process mining: A two-step approach to balance between underfitting and overfitting", *Softw. Syst. Model.*, **9**, 87-111. <https://doi.org/10.1007/s10270-008-0106-z>.
- Wang, Y., Zhao, X. and Wang, B. (2013), "LS-SVM and Monte Carlo methods based reliability analysis for settlement of soft clayey foundation", *J. Rock Mech. Geotech. Eng.*, **5**(4), 312-317. <https://doi.org/10.1016/j.jrmge.2012.06.003>.
- Wang, Z., Qiao, C., Song, C. and Xu, J. (2014), "Upper bound limit analysis of support pressures of shallow tunnels in layered jointed rock strata", *Tunn. Undergr. Sp. Tech.*, **43**, 171-183. <https://doi.org/10.1016/j.tust.2014.05.010>.
- Wong, K.S., Ng, C.W.W., Chen, Y.M. and Bian, X.C. (2012), "Centrifuge and numerical investigation of passive failure of tunnel face in sand", *Tunn. Undergr. Sp. Tech.*, **28**, 297-303. <https://doi.org/10.1016/j.tust.2011.12.004>.
- Xiang, Y.Z., Goh, A.T.C., Zhang, W.G. and Zhang, R.H. (2018), "A multivariate adaptive regression splines model for estimation of maximum wall deflections induced by braced excavation in clays", *Geomech. Eng.*, **14**(4), 315-324. <https://doi.org/10.12989/gae.2018.14.4.315>.
- Xu, J., Ren, Q. and Shen, Z. (2017), "Sensitivity analysis of the influencing factors of slope stability based on LS-SVM", *Geomech. Eng.*, **13**(3), 447-458. <https://doi.org/10.12989/gae.2017.13.3.000>.
- Yamamoto, K., Lyamin, A.V., Wilson, D.W., Sloan, S.W. and Abbo, A.J. (2011), "Stability of a circular tunnel in cohesive-frictional soil subjected to surcharge loading", *Comput. Geotech.*, **38**(4), 504-514. <https://doi.org/10.1016/j.compgeo.2011.02.014>.
- Zhang, B., Wang, X., Zhang, J.S. and Meng, F. (2017), "Three-dimensional limit analysis of seismic stability of tunnel faces with quasi-static method", *Geomech. Eng.*, **13**(2), 301-318. <https://doi.org/10.12989/gae.2017.13.2.301>.
- Zhang, H., Berg, A.C., Maire, M. and Malik, J. (2006), "SVM-KNN: Discriminative nearest neighbor classification for visual category recognition", *Proceedings of the IEEE Computer Society Conference on Computer Vision and Pattern Recognition*, New York, U.S.A., June.
- Zhang, P., Chen, R.P. and Wu, H.N. (2019), "Real-time analysis and regulation of EPB shield steering using random forest", *Autom. Constr.*, **106**, 102860. <https://doi.org/10.1016/j.autcon.2019.102860>.
- Zhang R.H., Zhang, W.G., Goh A.T.C., Hou, Z.J. and Wang, W. (2018), "A simple model for ground surface settlement induced by braced excavation subjected to a significant groundwater drawdown", *Geomech. Eng.*, **16**(6), 635-642. <https://doi.org/10.12989/gae.2018.16.6.635>.
- Zhang, W.G., Zhang, R.H., Fu, Y.R., Goh A.T.C. and Zhang, F. (2018), "2D and 3D numerical analysis on strut responses due to one-strut failure", *Geomech. Eng.*, **15**(4), 965-972. <https://doi.org/10.12989/gae.2018.15.4.965>.
- Zhang, W.G. and Goh A.T.C. (2016), "Evaluating seismic liquefaction potential using multivariate adaptive regression splines and logistic regression", *Geomech. Eng.*, **10**(3), 269-284. <https://doi.org/10.12989/gae.2016.10.3.269>.
- Zhang, W.G. and Goh A.T.C. (2014), "Multivariate adaptive regression splines model for reliability assessment of serviceability limit state of twin caverns", *Geomech. Eng.*, **7**(4), 431-458. <https://doi.org/10.12989/gae.2014.7.4.431>.

IC